

Mechanism of the Cyclopropanone Decarbonylation Reaction. A Density Functional Theory and Transient Spectroscopy Study

Andrei Poloukhine and Vladimir V. Popik*

Center for Photochemical Sciences, Bowling Green State University, Bowling Green, Ohio 43403

Received: November 3, 2005; In Final Form: December 2, 2005

The density functional theory analysis predicts that the thermal decarbonylation of cyclopropanones proceeds by the sequential and regioselective cleavage of both single bonds in a three-membered ring. The initial ring-opening process results in the formation of a reactive zwitterionic intermediate **6**, which is separated from the free alkyne and carbon monoxide by a very low energy barrier. Femtosecond pump–probe transient absorption spectroscopy experiments showed that light-induced decarbonylation is also a stepwise process but apparently proceeds on the excited-state surface. The lifetime of the intermediate in the photodecarbonylation reaction is very short and is dependent on substitution and solvent polarity. Thus, bis-*p*-anisyl-substituted species decays with $\tau = 0.6$ ps, bis- α -naphthyl-substituted intermediate has a lifetime of $\tau = 11$ ps, while the bis(2-methoxy-1-naphthyl)-substituted analogue survives for 83 ps in chloroform and for 168 ps in argon-saturated methanol. The loss of carbon monoxide from these intermediates results in the formation of corresponding acetylenes in an electronically ground state. The addition of triplet quenchers does not affect the dynamics or outcome of the reaction.

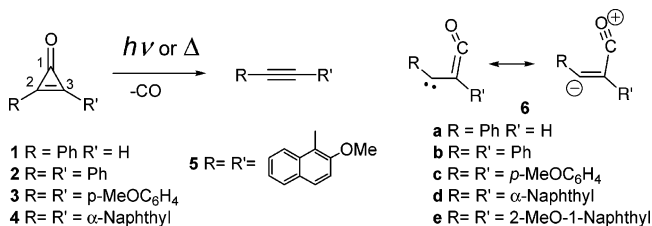
Introduction

Since its first preparation in 1959,¹ cyclopropanones received considerable attention due to their description as possible aromatic compounds.² The discovery of the cyclopropanone-containing natural antibiotic penitricin,³ as well as cyclopropanone-based protease inhibitors,⁴ renewed interest in this class of cyclic ketones. The three-membered ring of cyclopropanones is constructed of formally sp^2 -hybridized carbon atoms but is, nevertheless, characterized by high thermal stability.^{2,5} The chemical reactivity of cyclopropanones is dominated by two processes:² the nucleophilic ring opening, which results in the formation of acrylic acid derivatives,⁶ and the loss of carbon monoxide under high-temperature pyrolysis or in the presence of various catalysts.^{1b,7}

UV irradiation of cyclopropanones also results in a decarbonylation reaction and the formation of corresponding acetylenes^{6,8} (Scheme 1). This reaction often produces quantitative yields of alkynes and is characterized by a high quantum efficiency ($\Phi = 0.2–1.0$).^{5,8g}

Despite the widespread investigations of cyclopropanones, little is known about the mechanism of the decarbonylation reaction. In fact, very few examples of direct mechanistic studies of [2 + 1] retrocycloaddition reactions have been reported. The density functional theory (DFT) study of the hypothetical reverse process, the addition of carbon monoxide to a series of acetylenes ($HC\equiv CR$, where $R = H, F, OH, NH_2, CH_3,$ and Ph), suggested that the cycloaddition proceeds by the sequential formation of C–C bonds.⁹ Interestingly, the acyclic intermediate in this stepwise cycloaddition reaction was predicted to have an *E* arrangement of substituents. Its electronic structure can be described as a resonance hybrid of a ketylenylcarbene and a zwitterionic structure (**6**, Scheme 1). The loss of carbon

SCHEME 1



monoxide from bisketenes was also proposed to generate intermediate **6**, which then undergoes ring closure to form a cyclopropanone.¹⁰

While the thermodynamics of the photodecarbonylation reaction was studied in detail,¹¹ the data on the dynamics of this process remains controversial. A relatively long-lived ($\tau = 40$ ns) transient has been observed in the nanosecond laser flash photolysis of cyclopropanone **4**.⁵ On the other hand, picosecond experiments on diphenylcyclopropanone (**2**) suggested that the photodissociation is complete within the time resolution of an instrument (ca. 20 ps) and produces toluene in the T_1 state.¹² The latter results were recently confirmed by the femtosecond TUV absorption spectroscopy studies of **2**. Upon 267-nm excitation of the substrate, complex kinetics, including at least four processes, was observed in the picosecond time domain.¹³ The last transient was identified as an excited state of toluene, while the first very short lived transient was assigned to the S_2 state of **2** based on ground-state vibrational calculations. In contrast to these observations, some authors suggested that photodecarbonylation of cyclopropanones is a ground-state reaction of “hot” molecules rather than an excited-state process.⁹ This hypothesis was based on the fact that cyclopropanone vertical excitation energies calculated using time-dependent (TD) DFT and CIS methods were found to be much higher than the activation barrier for the decarbonylation step. Such a ground-state reaction, obviously, cannot produce triplet acetylene.

* To whom correspondence should be addressed. E-mail: vpopik@bgsnet.bgsu.edu.

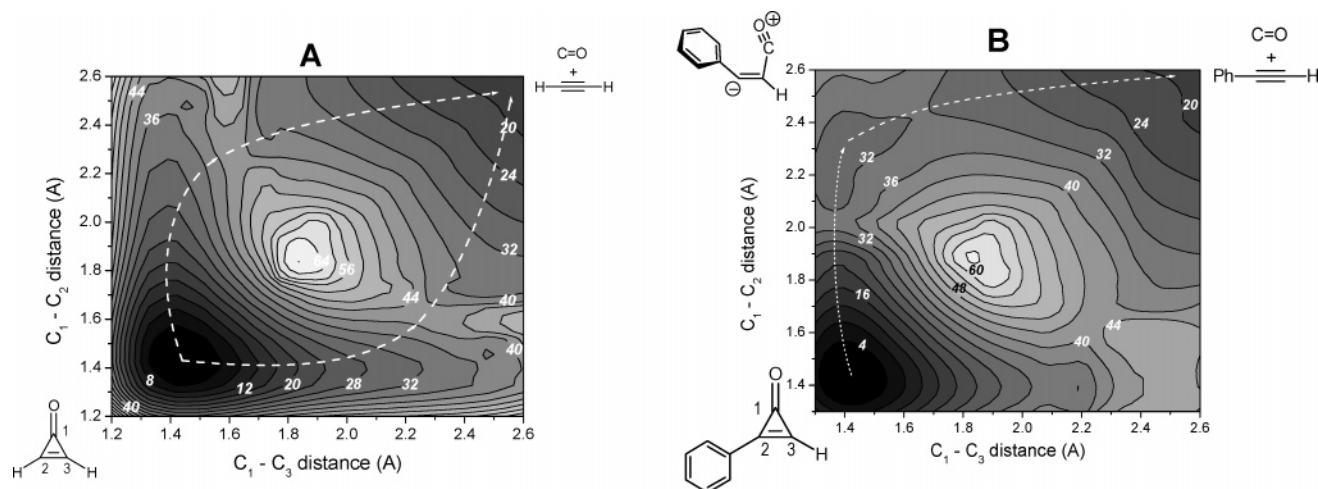


Figure 1. Contour plots of potential energy surfaces for the extrusion of carbon monoxide from parent cyclopropenone (A) and phenylcyclopropenone (B) calculated at B3LYP/6-31+G(d,p) level of theory. Numbers shown on the isoergic lines represent the relative energy in kcal/mol.

In this work we report a quantum-mechanical and time-resolved spectroscopic study of the decarbonylation reaction of diaryl-substituted cyclopropenones. Bis-*p*-anisylcyclopropenone (**3**) and two naphthyl-substituted cyclopropenones, bis(1-naphthyl)cyclopropenone (**4**) and bis(2-methoxy-1-naphthyl)cyclopropenone (**5**), were selected as the substrates for transient UV-Vis (TUV) and IR (TIR) experiments in order to satisfy the requirements of the femtosecond transient absorbance spectrometers used in this study.¹⁴ Quantum mechanical calculations were performed on phenyl- (**1**) and diphenylcyclopropenones (**2**) as well as bis-(4-hydroxyphenyl)cyclopropenone **3'**. Methoxy groups in **3'** were replaced with OH groups to simplify calculations. In our opinion, this modification should not significantly disturb the relative energies of the species involved in the transformations of **3**. Some calculations (at a lower level of theory) were also conducted for representative species of **4** and bis(2-hydroxy-1-naphthyl)cyclopropenone (**5'**).

Results and Discussion

Thermal Decomposition of Cyclopropenones **2**, **3**, and **5**.

Despite their high photochemical reactivity, diarylcyclopropenones are very stable compounds in the dark. In the absence of nucleophiles, these substrates show no signs of decomposition even after prolonged heating at 100 °C. Thermolysis of cyclopropenones **2**, **3**, and **5** was conducted by refluxing DMSO solutions (189 °C) of these compounds for 15–24 h. High-performance liquid chromatography (HPLC) analyses conducted during decomposition of **2** showed that only starting material and product were present in the reaction mixture during the course of the reaction and that no stable intermediates were observed. The corresponding acetylenes were the only isolatable products in this reaction (73% for **2**; 82% for **3**; and 87% for **5**), while the rest of the reaction mixture represented polyunsaturated polymeric material. The latter is apparently formed by thermal polymerization of acetylenes. In other words, the thermal decomposition of cyclopropenones results in a clean decarbonylation to acetylenes; however, it requires a relatively high temperature.

Theoretical Analysis of the Mechanism of the Thermal Decarbonylation Reaction. Geometries of the species involved in the decarbonylation of cyclopropenones **1**, **2**, and **3'** were preoptimized at the B3LYP/6-31+G(d,p) level and then re-optimized using the extended triple- ζ 6-311+G(3df,2p) basis set. Some structures were also optimized using the Hartree-

Fock (HF) method and 6-31+G(d,p) set. The 3-D relaxed potential-energy surface (PES) scans for the decarbonylation of phenylcyclopropenone (**1**), as well as parent cyclopropenone, were conducted at the B3LYP/6-31+G(d,p) level of theory in terms of C¹-C² and C¹-C³ distances (Scheme 1). The bottom-left corner of the contour plots corresponds to the energy of the starting cyclopropenone. Elongation of both C¹-C² and C¹-C³ bonds eventually leads to the release of carbon monoxide and the formation of an alkyne (upper-right corner).

The PES plot for the decarbonylation of parent cyclopropenone (Figure 1A) shows that the loss of carbon monoxide is a stepwise process. Synchronous cleavage of both C¹-C² and C¹-C³ bonds is unlikely since the simultaneous increase in both carbon-carbon distances results in a steep rise in energy. The valley on the PES follows the elongation of one of the C-C bonds, while the other bond remains virtually unchanged. Only when the first single bond of the cyclopropenone ring is almost broken (at ca. 2.2 Å), the cleavage of the second bond begins. The relaxed PES scan presented in Figure 1A does not show the formation of the intermediate; however, geometry optimization of the structure, which corresponds to the position on PES with coordinates 1.45 and 2.30 Å, allowed us to locate the energy minimum. This structure has a C¹-C² distance of 2.23 Å, a C¹-C³ of 1.36 Å, and is a real intermediate as frequency calculations found no imaginary frequencies. These results agree well with the previously reported DFT/CCSD study of the carbonylation of acetylene.⁹

The landscape of PES for the decarbonylation of phenylcyclopropenone (**1**, Figure 1B) also suggests the stepwise mechanism of carbon monoxide extrusion. In the case of compound **1**, single bonds in the cyclopropenone ring are not equal and the initial cleavage of the C¹-C² bond located next to the phenyl ring requires substantially less energy than the cleavage of the C¹-C³ bond. It is also interesting to note that the PES scan shown in Figure 1B clearly indicates that a rupture of the C¹-C² bond results in the formation of an intermediate **6a**. The latter then undergoes a dissociation of the C¹-C³ bond to form the final products, phenylacetylene and CO. The optimized geometries, as well as some representative structural parameters of cyclopropenones **1** and **2**, intermediates **6a** and **6b**, and transition states for the cleavage of the first (C¹-C², **1**^{TS1}, and **2**^{TS1}) and the second carbon-carbon bond (C¹-C³, **1**^{TS2} and **2**^{TS2}) are shown in Figure 2. The electronic energies of these structures are presented on the potential energy profiles for the decarbonylation of **1** and **2** (Figure 3).

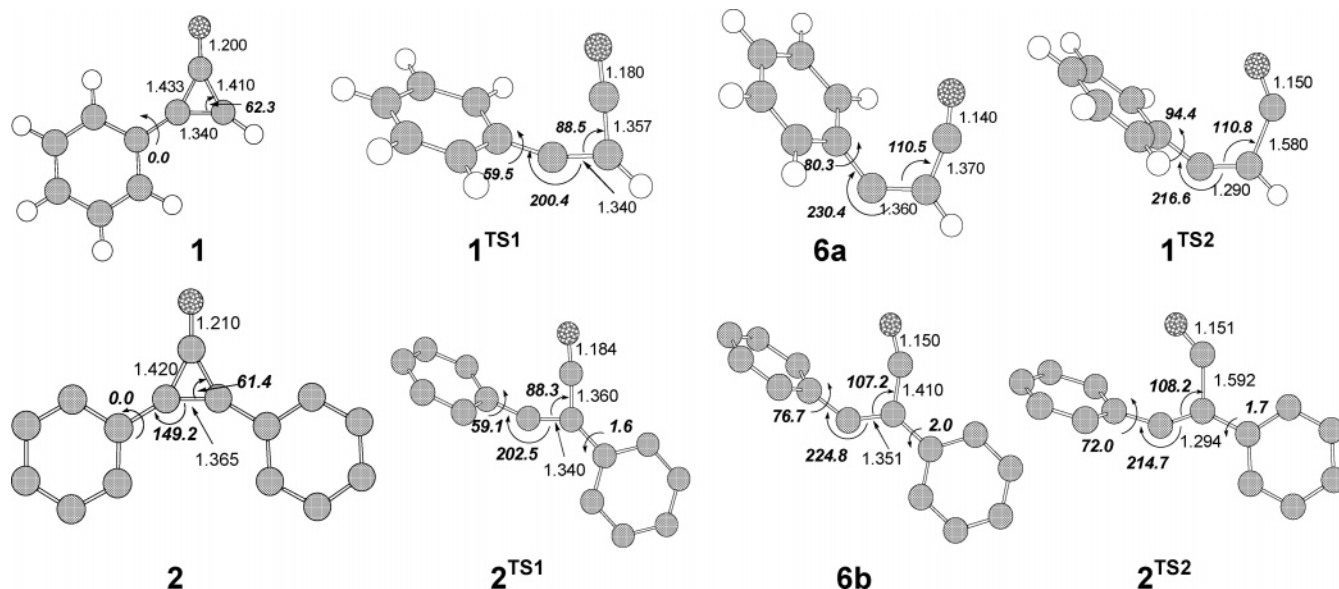


Figure 2. The B3LYP/6-311+G(3df,2p) optimized geometries of cyclopropenones **1** and **2**, ketenylcarbene intermediates **6a** and **6b**, and transition states for the cleavage of the first (C¹–C², **1^{TS1}** and **2^{TS1}**) and the second (C¹–C³, **1^{TS2}** and **2^{TS2}**) carbon–carbon bond. The bond distances are shown in angstroms, while bond angles and dihedral angles (highlighted in italics) are in degrees.

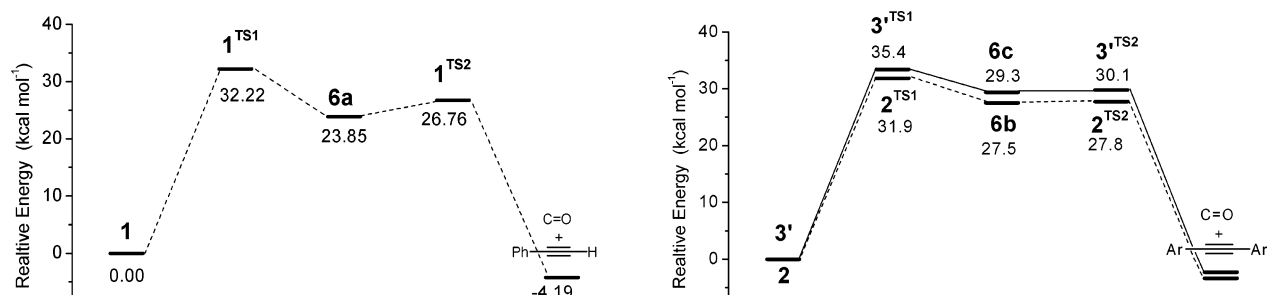


Figure 3. Schematic potential energy profile for the decarbonylation of phenylcyclopropenone (**1**), diphenylcyclopropenone (**2**), and bis(*p*-hydroxyphenyl)cyclopropenone (**3'**). Electronic energies were calculated at the B3LYP/6-311+G(3df,2p) level.

The phenyl substituents in substrates **1** and **2** lie in the plane of the cyclopropenone ring and both molecules are perfectly planar. The cleavage of the C¹–C² bond, and the formation of the intermediate **6** is accompanied by a substantial change in the molecular geometry. The phenyl group at C² moves from the *Z* arrangement with respect to the substituent at C³ in the starting material to a transoid position in ketenylcarbenes **6a** and **6b** (Figure 2). To verify the *E* geometry of **6a**, we have optimized the geometry of a *Z* isomer of **6a**, where the *Z* configuration was frozen, and found it to be 9 kcal/mol higher in energy than the *E*-**6a** at the B3LYP/6-31+G(d,p) level of theory. The *Z*-**6a** structure, however, does not correspond to a minimum on the PES. When structural restrictions are removed, the geometry optimization collapses to the starting cyclopropenone **1**. Geometry optimization of the *Z* analogue of the transition state structure **1^{TS2}** ultimately converges to **6a**. Furthermore, analysis of structures that correspond to the points along the reaction path, which is presented as a dotted line in Figure 1B, shows that *Z* to *E* dislocation of a substituent at C² proceeds in parallel with the elongation of the C²–C¹ bond. This displacement is accompanied by the rotation of the aromatic substituent around the C²–C^{Ar} bond. In the intermediate **6b**, the phenyl ring at C² is almost orthogonal to the C²–C³–C¹ plane. The other phenyl ring at C³ retains its coplanarity with the carbonyl group throughout the decarbonylation process.

As was mentioned above, the structure of the intermediate **6** can be described as a resonance hybrid of ketenylcarbene and zwitterion. We believe that the electronic structure of intermedi-

ate **6** is closer to the zwitterionic form since the ESP calculations predict a substantial negative charge on atom C² (–0.67 in **6a** and –0.53 in **6b**) and the length of the C²–C³ bond is very close to double bond values. In addition, it is known that in singlet arylcarbenes the aromatic ring is usually coplanar with the carbene,¹⁵ while in **6a** and **6b** the phenyl ring is almost orthogonal to that plane. This geometry can be explained by the conjugative stabilization of an unshared pair of electrons on the sp² orbital by the aromatic substituent at C². To test the potential diradical nature of intermediate **6a**, we conducted unrestricted UB3LYP/6-31+G(d,p) calculations. For the singlet multiplicity, we obtained a structure with the same geometry and same energy as in closed-shell calculations, as well as with zero spin. The triplet state of intermediate **6a** was found to be 10 kcal/mol higher in energy. Triplet **6a** can be described as a triplet phenylcarbene with a ketenyl substituent. The SOMO of this structure is a *p*-orbital at C² and the SOMO-1 is a σ orbital on the same atom. There is also some delocalization of the spin density into an aromatic ring and ketene moiety. We were unable to locate the saddle point on the triplet PES, which would lead to the decarbonylation and formation of the phenylacetylene. Overall, DFT calculations suggest that the ground state of intermediate **6** is singlet and that it reacts via the singlet manifold. The experimental observation that a triplet-sensitized photolysis of cyclopropenones produces the same product as the direct irradiation⁵ supports this suggestion.

Figure 3 summarizes the relative energies (starting cyclopropenones **1**, **2**, or **3'** were selected as the reference points in

respective reactions) for the loss of carbon monoxide from cyclopropanones **1**, **2**, and **3'** calculated at the B3LYP/6-311+G(3df,2p) level.

As can be seen in Figures 2 and 3, the loss of carbon monoxide from cyclopropanones **1**, **2**, and **3'** proceeds via sequential cleavage of C²–C¹ and C³–C¹ bonds. The rate-determining step in both cases is cleavage of the first (C²–C¹) carbon–carbon bond, which requires ca. 32–35 kcal/mol of activation energy (Figure 3). This value agrees well with the experimentally observed high thermal stability of cyclopropanones.⁵ The cleavage of the second (C³–C¹) bond and the loss of CO has a very low barrier and should proceed very rapidly. In fact, the PES between **6b** and **2**^{TS2}, as well as between **6c** and **3**^{TS2}, is virtually flat. It is interesting to note that the barrier for the loss of CO from the intermediate **6b** is predicted to be higher by correlative MP2 (2.7 kcal mol⁻¹, MP2(full)/6-311+G(d,p)) and HF (12.7 kcal mol⁻¹ HF/6-31+G(d,p)) methods than DFT. In addition, both DFT and HF calculations predict that ketenylcarbene intermediates **6a** and **6b** are real species as they are characterized by the minima on the corresponding PESs and have no imaginary frequencies. The phenyl substitution at C³ has little or no effect on the relative energies of transition states **TS1** and **TS2** but somewhat destabilizes the intermediate **6b**. Introduction of *p*-hydroxy substituents into the structure of diphenylcyclopropanone results in a weak stabilization of the initial cyclopropanone **3'** but has little effect on the relative stability of the intermediate **6c** (Figure 3). The DFT-optimized geometries of species involved in the decarbonylation of **3'** are very similar to those of **2** (Figure 2). Overall, the DFT calculations predict that decarbonylation of cyclopropanones is a stepwise process involving ketenylcarbene, zwitterionic intermediates **6**. The lifetime of these intermediates, however, is expected to be too short to allow for the detection or trapping in a thermal reaction.

Laser Flash Photolysis Studies. The irradiation of cyclopropanones **2**, **3**, **4**, and **5** in various solvents results in a quantitative conversion into the corresponding acetylenes. In previous picosecond¹² and femtosecond¹³ pump–probe laser flash photolyses of diphenylcyclopropanone (**2**), the formation of triplet diphenylacetylene (tolane) was detected. In our opinion, however, results of TUV experiments on **2** using 267-nm excitation should be treated with caution. The efficient decarbonylation reaction ($\Phi \approx 1$) is complete within a picosecond (vide infra) producing toluene, which has an extinction coefficient at 267 nm 3–4 times higher than that of starting material **2**. The 267-nm excitation of toluene produces a very strong signal, which is often difficult to separate from primary transients. In fact, in our femtosecond flash photolysis of diphenylcyclopropanone (**2**), we observed the signal of the S₁ state of toluene (formed within the time resolution of the instrument) even at the highest attainable flow rates (ca. 100 cm s⁻¹) of solution through a flow cell. An additional complication arises from the fact that transients produced on photolysis of **2** and triplet toluene have λ_{max} below 400 nm. As a result one has to rely on featureless tail absorption for the transient assignments.

In an attempt to shift the UV absorbance of the starting cyclopropanone and the intermediates involved in the decarbonylation reaction to a longer wavelength, we have prepared three cyclopropanones bis-*p*-anisylcyclopropanone (**3**), bis(1-naphthyl)cyclopropanone (**4**), and bis(2-methoxy-1-naphthyl)cyclopropanone (**5**). The changes in the UV spectrum associated with decarbonylation of **5** are shown in Figure 4. The UV spectra of cyclopropanones **3** and **4**, as well as of corresponding acetylenes, were reported previously.^{5,16} The dynamics of the

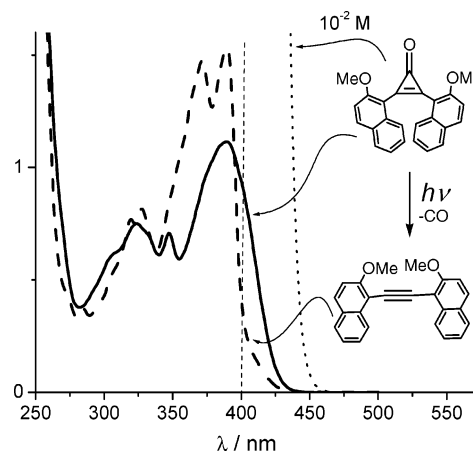


Figure 4. UV spectra of cyclopropanone (**5**, 5×10^{-5} M, solid line, and 10^{-2} M, dotted line) and bis(2-methoxynaphth-1-yl) acetylene (5×10^{-5} M, dashed line) in methanol.

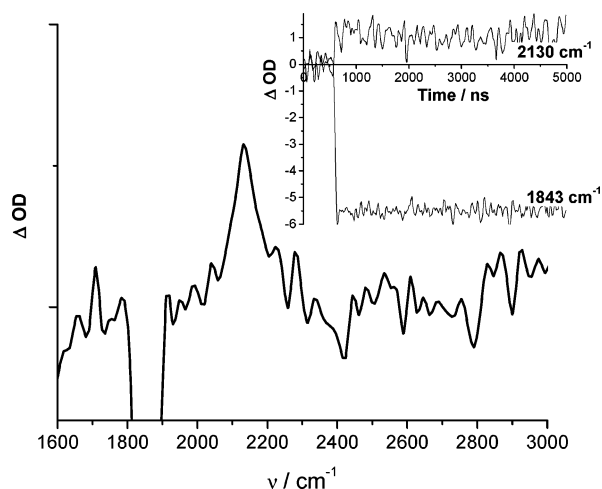


Figure 5. TIR difference spectrum observed from 0 to 30 ns following 355-nm laser photolysis of cyclopropanone (**5**) in CCl₄. Insert shows kinetic traces observed at 1843 cm⁻¹ (starting material, **5**) and 2130 cm⁻¹ (carbon monoxide).

photochemically induced decomposition of diaryl-substituted cyclopropanones were studied by both TIR and TUV spectroscopies in the nanosecond and picosecond time domains.

Nanosecond TIR spectroscopic study¹⁷ of bis(2-methoxynaphth-1-yl)-cyclopropanone (**5**) was conducted in carbon tetrachloride solutions. The TIR difference spectrum obtained from 0 to 30 ns after the 355-nm laser pulse is shown in Figure 5.

The laser irradiation of the ca. 4 mM solution of bis(2-methoxynaphth-1-yl)-cyclopropanone (**5**) in carbon tetrachloride results in instantaneous (on the time scale of the instrument) bleaching of the starting material. This can be observed as a strong negative band at ca. 1843 cm⁻¹ (Figure 5). This bleaching is accompanied by the instant formation of a broad absorbance band at ca. 2130 cm⁻¹, which corresponds to the ν_{CO} frequency of carbon monoxide.^{8g} The intensity of both the negative and the positive bands in the difference spectrum remains constant for the duration of the experiment (5 μs , insert in Figure 5). This observation allowed us to conclude that the decarbonylation of the cyclopropanone **5** is complete within 30 ns after the laser pulse.

Femtosecond TUV pump–probe photolysis of cyclopropanones **3**, **4**, and **5** allowed us to detect a very rapid formation and then a somewhat slower decay of a short-lived intermediate. The rise of a transient spectrum, which is complete in ca. 400

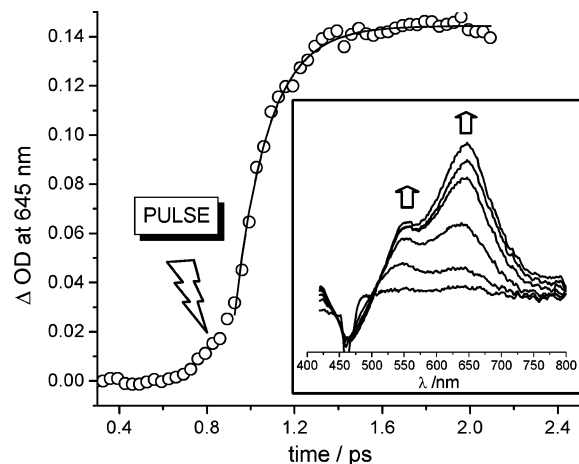


Figure 6. The formation of a transient spectrum induced by 90-fs pulsed photolysis of ca. 0.23 mM solution of **5** in Ar saturated methanol. The insert shows changes in the difference UV-vis spectrum recorded every 50 fs after the pulse (spectra are not corrected for “chirp”).

TABLE 1: Lifetimes for the Formation and Decay of Transients Produced in Photolysis of Cycloproponones 3, 4, and 5 in Various Solvents

	solvent	λ_{\max}/nm	$\tau_{\text{RISE}}/\text{fs}^c$	τ_1/ps^c
3 ^a	MeOH/Ar ^d	454	350 ± 160	0.624 ± 0.036
4 ^a	CHCl ₃ /Ar ^d	628	163 ± 31	10.8 ± 0.3
5 ^b	<i>n</i> -pentane/CH ₂ Cl ₂ (7:3)	649	194 ± 21	38.9 ± 1.0
	CHCl ₃	658	214 ± 47	83.4 ± 1.0
	CH ₃ CN	644	234 ± 14	74.4 ± 1.5
	MeOH/Ar ^d	639	232 ± 9	168.1 ± 2.7
			(268 ± 16) ^e	
	MeOH/O ₂ ^f	639	246 ± 74	162.1 ± 1.4
			(266 ± 13) ^e	
	MeOH/1,3-C ₆ H ₈ ^g	641	219 ± 23	165.2 ± 4.1

^a $\lambda_{\text{excitation}} = 267 \text{ nm}$. ^b $\lambda_{\text{excitation}} = 400 \text{ nm}$. ^c The formation and the decay of the intermediate were followed at 454 nm for **3**, 630 nm for **4**, and 645 nm for **5**. ^d Argon was constantly bubbled through a solution during experiment. ^e The lifetime of the excited state shown in parentheses was measured from the decay signal at 500 nm. ^f Oxygen was constantly bubbled through a solution. ^g In the presence of 23 mM 1,3-cyclohexadiene.

fs following a 94-fs pulsed irradiation of cycloproponone **5** at 400 nm, is shown in Figure 6.

The formation of transient spectra with a similar rise-time were observed in the photolysis of bis-*p*-anisylcycloproponone (**3**) and bis(1-naphthyl)cycloproponone (**4**) in methanol. The formation rate of intermediate is virtually independent of the solvent polarity and the presence or absence of various additives (Table 1).

The dynamics of bis-*p*-anisylcycloproponone (**3**) decarbonylation was studied using 267-nm pump pulses. Similar excitation of **2** produced complex dynamics interpreted by the authors as $S_2 \rightarrow S_1 \rightarrow S_{1(\text{tolane})} \rightarrow T_{1(\text{tolane})}$ sequence. The major difference between cycloproponones **3** and **2** is that the former has a stronger absorbance at 267 nm than the bis-*p*-anisylacetylene, therefore reducing the probability of secondary photochemistry. The transient spectrum formed in the 94-fs pulsed photolysis of **3** at 267 nm in methanol is shown in Figure 7. It has a maximum at $\lambda = 454 \text{ nm}$ and a weaker band at ca. 665 nm. The decay of this transient follows simple first-order kinetics with a lifetime of $\tau = 0.624 \pm 0.036 \text{ ps}$ in argon-saturated methanol. No observable transients are produced in the UV-vis range (Figure 7).

The direct 267-nm excitation of bis-*p*-anisylacetylene results in the formation of a very different transient spectrum

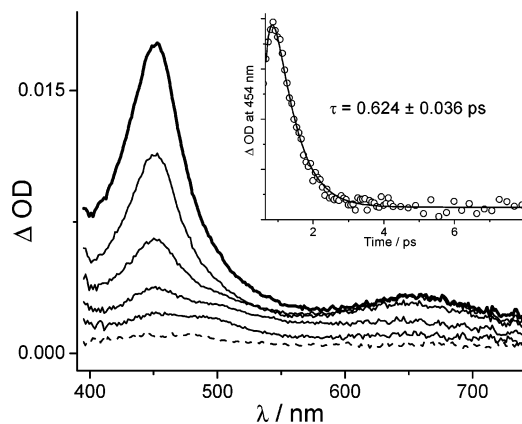


Figure 7. Transient spectra recorded every 0.4 ps (solid lines) following 267-nm excitation of cycloproponone (**3**) in methanol. The spectrum represented with a dashed line was recorded 10 ps after the pulse. Insert shows a kinetic trace observed at 454 nm. Curve represents the calculated fit to a double exponential equation.

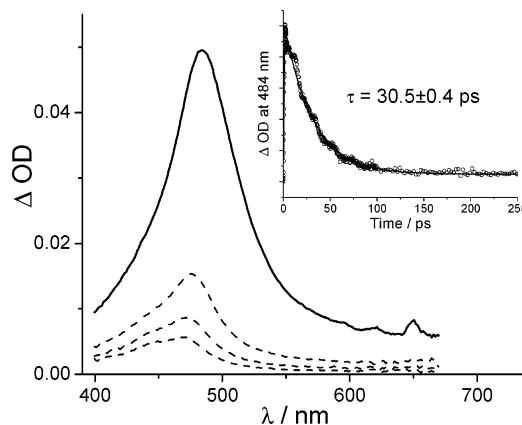


Figure 8. Transient spectra recorded every 40 ps following 267-nm excitation laser photolysis of bis-*p*-anisylacetylene in methanol. Insert shows a kinetic trace observed at 484 nm. Curve represents the calculated fit to a double exponential equation.

with $\lambda_{\max} = 484 \text{ nm}$ (Figure 8). This transient has a lifetime of $\tau = 30 \text{ ps}$ in argon-saturated methanol and can be assigned to the S_1 state of the acetylene.¹⁸ The relatively long lifetime of S_1 bis-*p*-anisylacetylene allows us to conclude that the excitation of bis-*p*-anisylcycloproponone (**3**) does not result in the formation of corresponding acetylene in an electronically excited state.

The 400-nm excitation of cycloproponone **5** in argon-saturated methanol produces a transient spectrum, which shows a maximum at $\lambda = 639 \text{ nm}$, a shoulder at ca. 550 nm, and a negative absorbance band at 467 nm (Figure 9). A similar spectrum with λ_{\max} at ca. 628 nm is produced upon irradiation of bis- α -naphthylcycloproponone (**4**) (Figure 10). It is interesting to note that the λ_{\max} value of the transient spectrum produced in the photolysis of **5** is solvent dependent and shows a 10–19-nm red shift in nonpolar aprotic solvents (Table 1).

The decay of both transients is complete within 0.5 ns and does not result in the formation of any new absorbance in the visible spectrum. The transient spectrum produced upon photolysis of **5** shows a clean isosbestic point at 505 nm (Figure 9). The decay of this transient is concomitant with the growth of absorbance at 380 nm, which corresponds to the ground state of bis(2-methoxy-1-naphthyl)acetylene (insert in Figure 11). The direct excitation of the bis(2-methoxynaphth-1-yl)acetylene produces a long-lived ($\tau > 10 \text{ ns}$) transient spectrum (Figure

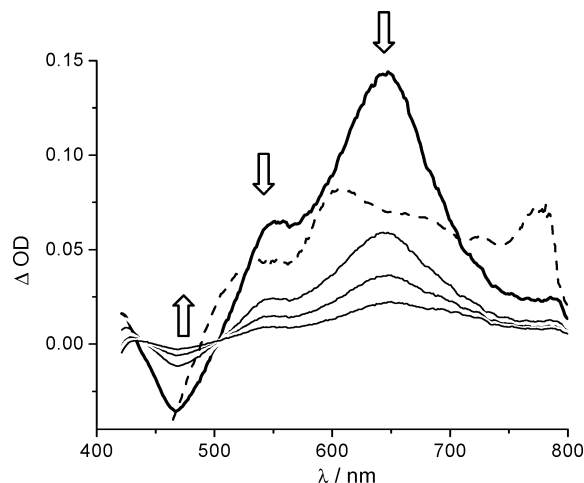


Figure 9. Transient spectrum recorded 1 ps after the 90-fs 400-nm pulsed laser photolysis of cyclopropanone **5** in Ar-saturated methanol (solid line, subsequent spectra were recorded every 80 ps). Spectrum produced in photolysis of bis-(2-methoxynaphth-1-yl) acetylene is shown as a dashed line.

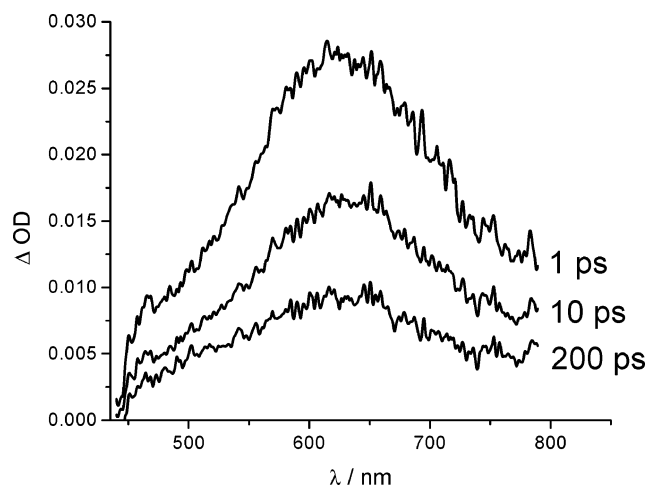


Figure 10. Transient spectrum recorded in photolysis of cyclopropanone **4** in Ar-saturated methanol.

9), which is assigned to a T_1 state of the alkyne (vide infra). We can conclude that, as is in the case of bis-*p*-anisyl cyclopropanone **3**, the decarbonylation of cyclopropanone **5** produces the ground state of the corresponding alkyne.

The interesting feature of the transient spectrum shown in Figure 9 is a negative absorbance at 467 nm, which cannot be explained by bleaching of the starting material **5** since the latter does not absorb at this wavelength (Figure 4). In addition, the growth of absorbance at 467 nm occurs at the same rate as the decay at 639 and 550 nm. These observations suggest that the negative absorbance comes from the probe-pulse-induced emission of the transient, meaning that the intermediate produced in the photolysis of cyclopropanone **5** is formed in an electronically excited state of singlet multiplicity.¹⁹ Similar induced emission bands at ca. 470 nm were observed in transient spectra produced upon photolysis of **5** in other solvents (acetonitrile, chloroform, and pentane–methylene chloride mixtures). However, we have not seen strong negative bands in the transient spectra of cyclopropanones **1–4**, apparently due to the fact that such band should lie ca. 170 nm to the blue from the major absorbance band. For compounds **2** and **3**, it would appear below the short-wavelength limit of our spectrometer (400 nm), while for the bis- α -naphthylcyclopropanone (**4**), the weak emission band overlaps with the laser pulse.

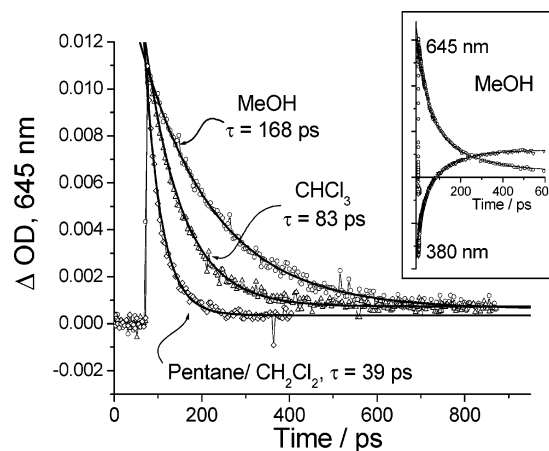


Figure 11. Kinetic traces observed at 645 nm in argon-saturated methanol (circles), chloroform (triangles), and pentane–dichloromethane mixture (squares) following 400-nm pulsed laser photolysis of **5**. The insert illustrates growth of absorbance at 380 nm, which is concomitant to the decay of the transient absorbance at 650 nm. Curves represent the calculated fit to a single-exponential equation.

The lifetime of the transient produced in 400 nm photolysis of **5** strongly depends on solvent polarity (Figure 11, Table 1). Thus, decay of this transient in methanol is more than four times slower than in a pentane–methylene chloride mixture.

MO Analysis of the Photodecarbonylation Reaction. The properties of frontier orbitals in all of the cyclopropanones studied (**1–5**) are very similar. The HOMO and HOMO-1 are very close in energy and are mostly localized on the carbonyl oxygen (Figure 12). The HOMO lies in the plane of the ring, while HOMO-1 is orthogonal to that plane. The major component of the LUMO, on the other hand, is an antibonding π^* orbital of an endocyclic double bond. In aryl-substituted cyclopropanones, the LUMO has also substantial coefficients on aromatic carbons.

According to TD DFT calculations, cyclopropanones **2**, **3**, and **4**, as well as the parent cyclopropanone, have two closely lying singlet excited states.²⁰ Both can be approximated as $n \rightarrow p^*$ states. S_1 is produced mostly by the HOMO \rightarrow LUMO transition and is a symmetry-forbidden excitation, which is reflected in a very low oscillator strength (Table S1). The weak $S_0 \rightarrow S_1$ band is not usually visible in the electronic spectra of diarylcyclopropanones,⁵ because of its overlap with a much stronger $S_0 \rightarrow S_2$ absorbance (e.g., Figure 4). In fact, we were able to observe a very weak ($\log \epsilon \approx 0.3$) longer wavelength band only in solutions of diphenylcyclopropanone (**2**) and only in nonpolar solvents. The HOMO-1 \rightarrow LUMO is a symmetry-allowed transition and is characterized by an almost 4 orders of magnitude increase in oscillator strength. The $S_0 \rightarrow S_2$ absorbance, therefore, has a higher extinction coefficient ($\log \epsilon = 4–4.5$).

The Nature of the Transient. Two mechanisms of photochemical decarbonylation of cyclopropanones have been discussed in the literature. One group suggested that photochemical decarbonylation of cyclopropanones is a ground-state process, which just utilizes the energy of electronic excitation to cross the ground-state activation barrier. We believe that experimental data contradicts this hypothesis. The short-lived species observed in the femtosecond photolysis of cyclopropanones **3–5** are formed within 150–350 fs. According to the Energy Gap Law,²¹ the rate of $S_1 \rightarrow S_0$ internal conversion (k_{IC}) for **5** should be around 10^7 s^{-1} and even slower for cyclopropanones **3–4**. The upper limit for radiationless deactivation of the $S_n \rightarrow S_0$ state is ca. 10^{11} s^{-1} .²¹ In other words, the rate of formation of the

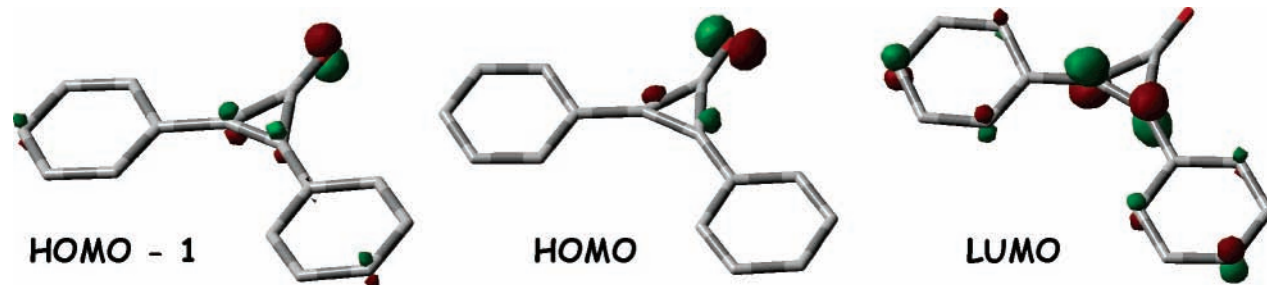


Figure 12. Graphical representation of frontier molecular orbitals of diphenylcycloproponone **2** calculated at B3LYP/6-311+G(3df,2p) level.

transient is too fast to be explained by the internal conversion to the ground state of cycloproponone. In addition, the UV–vis spectra of the transients are very different from the ground-state spectra of cycloproponones **3–4**. Finally, radiationless return to the ground state of the cycloproponone before the transition state of the decarbonylation reaction (**TS1**) is unlikely to result in quantum yields close to unity, which were observed experimentally for **2**. Assignment of the ground-state intermediate structure **6** to the observed transient is also unlikely since excited cycloproponone has to undergo bond cleavage and dissipate remaining ca. 40 kcal mol⁻¹ energy within few molecular vibrations.²² Therefore, we can conclude that the transient is formed in an electronically excited state. The observed stimulated emission provides strong support for this conclusion (Figure 9).

It has been also suggested that the transient in question is the S₁ state of cycloproponone, which is produced by the rapid internal conversion from some higher excited state.¹³ This assignment cannot explain the substantial dependence of the transient lifetime on the solvent polarity (Figure 11). In addition, the difference between the maxima in the emission (negative band in Figure 9) and absorbance spectra (Figure 4) gives a Stokes shift of ca. 4500 cm⁻¹. This value corresponds to ca. 13 kcal mol⁻¹ of S₁ vibrational relaxation energy, which is, in our opinion, too high for a rigid diarylcyclopropane molecule. Finally, cycloproponone **5** was excited by the irradiation into the lowest energy absorption band, which should correspond to S₀ → S₁ excitation.

In other words, experimental data suggest that the excitation of diarylcycloproponones results in the very rapid formation of the intermediate in its electronically excited state. This intermediate loses carbon monoxide to produce corresponding acetylene in an electronically ground state. The strong stabilization of this intermediate by polar solvents (Figure 11, Table 1) allows us to suggest that the photochemically produced transient has a zwitterionic structure similar to its ground-state counterpart **6**.

Nanosecond Flash Photolysis. The femtosecond pump–probe transient spectroscopy experiments on cycloproponones **3**, **4**, and **5** clearly indicate that the photochemical decarbonylation of these substrates is complete within less than a nanosecond. However, we⁵ and others¹² have reported that pico- and nanosecond flash photolysis of cycloproponones results in the formation of a transient with a lifetime in the nanosecond time domain. The 355-nm nanosecond laser flash photolysis of cycloproponone **5** also allowed us to observe a strong transient signal with absorbance maximum at ca. 600 nm (Figure 13). The decay lifetime of this transient in argon-saturated methanol is 471 ± 2.8 ns. The addition of triplet quenchers, such as 21 mM of 1,3-cyclohexadiene, or saturation of solution with oxygen results in a substantial increase in the rate of decay ($\tau_{(\text{CYCLOHEXADIENE})} = 167.3 \pm 0.1$ ns and $\tau_{(\text{O}_2)} = 60.4 \pm 0.3$ ns), suggesting the triplet multiplicity of the transient

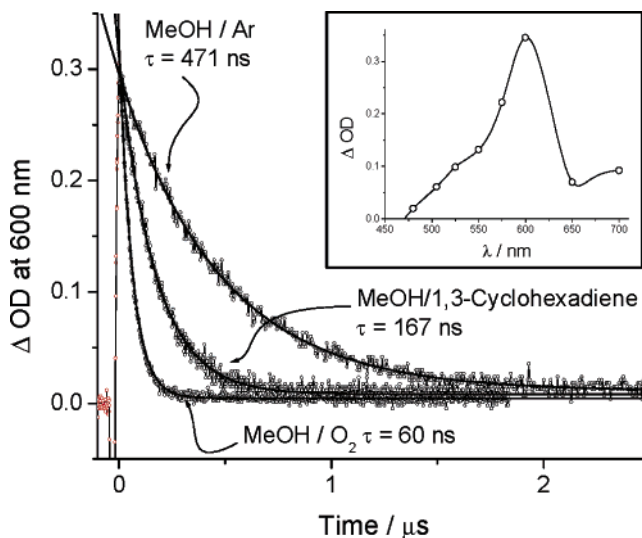


Figure 13. Kinetic traces observed at 600 nm following 355-nm pulsed laser photolysis of **5** in argon-saturated methanol, oxygen-saturated methanol, and in the presence of 21 mM of 1,3-cyclohexadiene. Insert shows the spectrum of this transient reconstructed from kinetic traces at different wavelength. Curves represent the calculated fit to a single-exponential equation.

species (Figure 13). We were quite puzzled by this observation, since TIR data shows that the decarbonylation reaction is complete within the nanosecond laser pulse (Figure 5). On the other hand, decay of the picosecond transient does not produce any new species absorbing at ca. 600 nm (Figure 9). We also found that continuous flashing of the cell with the stopped flow pump, which results in rapid bleaching of the starting cycloproponone **5**, was in fact producing the increasingly stronger signal, which eventually saturated. Analysis of the reaction mixture at this point indicated a complete absence of the starting material. To the contrary, the major component of reaction mixture (above 90%) was bis(2-methoxy-1-naphthyl)acetylene. Finally, when the methanol solution of the latter was irradiated at 355 nm, we observe a signal identical in intensity and decay rate to the one observed in the bleached solution of **5**. The decay of the transient produced by the laser flash photolysis of bis(2-methoxy-1-naphthyl)acetylene shows the same dependence on the concentration of 1,3-cyclohexadiene or oxygen. The femtosecond TUV experiments showed that excitation of this alkyne results in a very rapid (ca. 1 ps) formation of a transient spectrum with $\lambda_{\text{max}} = 608$ nm (dashed line in Figure 9). This transient shows very slow decay (less than 10% in 1.5 ns) and apparently corresponds to a triplet excited state of bis(2-methoxy-1-naphthyl)acetylene.

Taking into account the fact that the decarbonylation reaction of **5** is complete within a nanosecond, the duration and the intensity of the Nd:YAG laser pulse (5 ns, 30 mJ pulse⁻¹ at 355 nm) and the fact that bis(2-methoxy-1-naphthyl)acetylene

has somewhat higher absorbance at 355 nm than the starting material (Figure 5), we can assume that the nanosecond signal is due to the secondary excitation of the product formed within the duration of the laser pulse.

Conclusions

We have shown that photochemical and thermal decarbonylation of cyclopropanones is a stepwise process. In a thermal reaction, the initial cleavage of one of the single bonds in the cyclopropanone ring results in the formation of an intermediate **6**, which electronic structure can be described as a resonance hybrid of ketylenylcarbene and zwitterion. The DFT calculations suggest the presence of a substantial charge separation in **6**, supporting a major contribution from the zwitterionic structure. While the cleavage of the first carbon-carbon bond in cyclopropanones requires ca. 32 kcal mol⁻¹, the barrier for the decarbonylation of **6** is very low, making intermediate **6** a very short-lived species.

The photochemical decarbonylation of cyclopropanones apparently proceeds on the excited-state energy surface. The excitation of cyclopropanones **3**, **4**, and **5** results in the very rapid formation of an intermediate in an electronically excited state. The effect of solvent polarity on the spectra and lifetime of this intermediate allows us to propose a zwitterionic structure similar to the ground-state counterpart. The decay of this intermediate produces a ground-state alkyne.

Experimental Section

Materials. The preparation of bis-*p*-anisylcyclopropanone (**3**), bis- α -naphthylcyclopropanone (**4**), as well as bis(2-methoxy-1-naphthyl)cyclopropanone (**5**) by Friedel-Crafts alkylation of the corresponding naphthalenes with trichlorocyclopropenium cation followed by hydrolysis of the resulting 1,1-dichlorocyclopropanes, as well as spectral data for these compounds, has been described previously.⁵ Chloroform and dichloromethane were distilled from phosphorus pentoxide under argon immediately before use. Pentane was distilled from sodium. HPLC-grade methanol was obtained from Fisher.

Photolytic Experiments. Analytical photolyses were performed by the irradiation of ca. 10⁻⁴ M solutions of cyclopropanones in a 1-cm quartz cell using a RMR-600 Rayonet photochemical reactor equipped with a carousel and a set of eight lamps with λ_{max} at 350 nm. Reaction mixtures were then analyzed by HPLC. Preparative photolyses were conducted by the irradiation of methanol solutions of c.a. 100 mg of cyclopropanones using 16 lamp (with $\lambda_{\text{emission}} = 350$ nm) Rayonet photochemical reactor in a quartz vessel equipped with an immersible cooling finger. Consumption of the starting material was followed by thin-layer chromatography. After the irradiation, solvent was removed in a vacuum and products were analyzed by NMR spectroscopy. The NMR spectra showed quantitative formation of corresponding acetylenes. The nanosecond TUV and TIR laser flash photolysis experiments were carried out using a frequency tripled (355 nm) output of a Q-switched Nd:YAG laser as the excitation source. The setup of the laser system and time-resolved UV spectrometer,²³ as well as step-scan Fourier transform infrared (FTIR) setup,¹⁷ were described previously. The femtosecond TUV experiments were conducted using an ultrafast pump-probe instrument based on Ti:Sapphire laser.¹⁴ In the current experiments excitation was at 267 or 400 nm (the third and second harmonic of the Ti-Sapphire output).

Theoretical Procedures. Density functional theory calculations were carried out using the Gaussian 98 program.²⁴

Geometries were preoptimized using a B3LYP hybrid functional and 6-31+G(d,p) basis set and then reoptimized using extended triple- ζ basis at the B3LYP/6-311+G(3df,2p) level. Zero-point vibrational energy (ZPVE) corrections, required to correct the raw relative energies to 0 K, were obtained from B3LYP/6-311+G(3df,2p) frequency calculations. Analytical second derivatives were computed to confirm each stationary point to be a minimum by yielding zero imaginary vibrational frequencies. These frequency analyses are known to overestimate the magnitude of the vibrational frequencies. Therefore, we scaled the frequencies by 0.9772.²⁵ The IRC calculations for transition states and relaxed scans of potential energy surfaces were conducted at the B3LYP/6-31+G(d,p) level. In the PES scans, the C²-C¹ and C³-C¹ coordinates were fixed in steps, while the other degrees of freedom were fully optimized. Each of the two potential energy surfaces consisted of about 200 points, corresponding to different values of C²-C¹ and C³-C¹ distances. The vertical excitation energies were evaluated using the Random Phase Approximation for a TD DFT calculation method, at the TD-B3PW91/6-311++G(3df,2p) level.

Acknowledgment. Authors would like to thank Professor Michael A.J. Rodgers for useful discussions, Dr. Evgeny O. Danilov for the assistance in conducting TIR and TUV experiments, and the Ohio Laboratory for Kinetic Spectroscopy for the use of instrumentation. We are grateful to the National Institutes of Health (CA91856-01A1) and National Science Foundation (CHE-0449478) for the support. A.P. thanks the McMaster Endowment for the research fellowship.

Supporting Information Available: UV Spectra of cyclopropanones **2**–**4**, results of TD DFT calculations, Gaussian 98 output files for DFT calculations, and complete ref 20 (PDF). This material is available free of charge via the Internet at <http://pubs.acs.org>.

References and Notes

- (1) (a) Breslow, R.; Haynie, R.; Mirra, J. *J. Am. Chem. Soc.* **1959**, *81*, 247. (b) Vol'pin, M. E.; Koreskov, Y. D.; Kursanov, D. N. *Dokl. Akad. Nauk SSSR, Ser. Khim.* **1959**, 506.
- (2) Komatsu, K.; Kitagawa, T. *Chem. Rev.* **2003**, *103*, 1371. Potts, K. T.; Baum, J. S. *Chem. Rev.* **1974**, *74*, 189. Halton, B.; Banwell, M. G. In *The Chemistry of Cyclopropyl Group*; Rappoport, Z., Ed.; Wiley: New York, 1987; p 1300.
- (3) Okuda, T.; Yoneyama, Y.; Fujiwara, A.; Furumai, T. *J. Antibiotics* **1984**, *37*, 712.
- (4) (a) Ando, R.; Morinaka, Y.; Tokuyama, H.; Isaka, M.; Nakamura, E. *J. Am. Chem. Soc.* **1993**, *115*, 1515. (b) Ando, R.; Sakaki, T.; Morinaka, Y.; Takahashi, C.; Tamao, Y.; Yoshii, N.; Katayama, S.; Saito, K.; Tokuyama, H.; Isaka, M.; Nakamura, E. *Bioorg. Med. Chem.* **1999**, *7*, 571.
- (5) Poloukhine, A.; Popik, V. V. *J. Org. Chem.* **2003**, *68*, 7833.
- (6) Dehmlow, E. V.; Neuhaus, R.; Schell, H. G. *Chem. Ber.* **1988**, *121*, 569. Dehmlow, S. S.; Dehmlow, E. V. *Z. Naturforsch. B* **1975**, *30b*, 404. Dehmlow, E. V. *Leib. Ann.* **1969**, 729, 64; Ciabattani, J.; Nathan, E. C. *J. Am. Chem. Soc.* **1969**, *91*, 4766.
- (7) Wadsworth, D. H.; Donatelli, B. A. *Synthesis* **1981**, 285. Breslow, R.; Eischer, T.; Krebs, A.; Peterson, R. A.; Posner, J. *J. Am. Chem. Soc.* **1965**, *87*, 1320.
- (8) (a) Chiang, Y.; Kresge, A. J.; Popik, V. V. *J. Am. Chem. Soc.* **1999**, *121*, 5930. (b) Chiang, Y.; Kresge, A. J.; Paine, S. W.; Popik, V. V. *J. Phys. Org. Chem.* **1996**, *9*, 361. (c) Chiang, Y.; Kresge, A. J.; Popik, V. V. *J. Am. Chem. Soc.* **1995**, *117*, 9165. (d) Wagner, B. D.; Zgierski, M. Z.; Luszyk, J. *J. Am. Chem. Soc.* **1994**, *116*, 6433. (e) Murata, S.; Yamamoto, T.; Tomioka, H. *J. Am. Chem. Soc.* **1993**, *115*, 4013. (f) Krebs, A.; Cholcha, W.; Mueller, M.; Eicher, T.; Pielartzik, H.; Schnoekel, H. *Tetrahedron Lett.* **1984**, *25*, 5027. (g) Fessenden, R. W.; Carton, P. M.; Shimamori, H.; Scaiano, J. C. *J. Phys. Chem.* **1982**, *86*, 3803. (h) Chapman, O. L.; Gano, J.; West, R. P.; Regitz, M.; Maas, G. *J. Am. Chem. Soc.* **1981**, *103*, 7033. (i) Quinkert, G.; Opitz, K.; Wiersdorff, W. W.; Weinlich, J. *Tetrahedron Lett.* **1963**, 1863.

- (9) Nguyen, L. T.; De Proft, F.; Nguyen, M. T.; Geerlings, P. *J. Org. Chem.* **2001**, *66*, 4316. Nguyen, L. T.; De Proft, F.; Nguyen, M. T.; Geerlings, P. *J. Chem. Soc. Perkin Trans. 2* **2001**, 898.
- (10) Sung, K.; Fang, D. C.; Glenn, D.; Tidwell, T. T. *J. Chem. Soc. Perkin Trans. 2* **1998**, 2073. Dailey, W. P. *J. Org. Chem.* **1995**, *60*, 6737; Demhlow, E. V. *Tetrahedron Lett.* **1972**, 1271.
- (11) Schmidt, R. *J. Phys. Chem. A* **1998**, *102*, 9082. Schmidt, R.; Schuetz, M. *Chem. Phys. Lett.* **1996**, *263*, 795. Hara, T.; Hirota, N.; Terazima, M. *J. Phys. Chem.* **1996**, *100*, 10194. Hung, R. R.; Grabowski, J. J. *J. Am. Chem. Soc.* **1992**, *114*, 351. Herman, M. S.; Goodman, J. L. *J. Am. Chem. Soc.* **1989**, *111*, 1849. Grabowski, J. J.; Simon, J. D.; Peters, K. S. *J. Am. Chem. Soc.* **1984**, *106*, 4615.
- (12) Hirata, Y.; Mataga, N. *Chem. Phys. Lett.* **1992**, *193*, 287.
- (13) Takeuchi, S.; Tahara, T. *J. Chem. Phys.* **2004**, *120*, 4768.
- (14) The pump-probe instrument for the femtosecond transient absorption measurements was described in: Nikolaitchik, A. V.; Korth, O.; Rodgers, M. A. J. *J. Phys. Chem. A* **1999**, *103*, 7587. Some additional modifications were reported in: Pelliccioli, A. P.; Henbest, K.; Kwag, G.; Carvagno, T. R.; Kenney, M. E.; Rodgers, M. A. J. *J. Phys. Chem. A* **2001**, *105*, 1757.
- (15) Karney, W. L.; Borden, W. T. *J. Am. Chem. Soc.* **1997**, *119*, 1378; Matzinger, S.; Bally, T.; Patterson, E. V.; McMahon, R. J. *J. Am. Chem. Soc.* **1996**, *118*, 1535; Zhu, Z. D.; Bally, T.; Stracener, L. L.; McMahon, R. J. *J. Am. Chem. Soc.* **1999**, *121*, 2863.
- (16) UV spectra of compounds **2–4** are presented in Supporting Information.
- (17) The step-scan FTIR setup used in this work was described previously: Fedorov, A. V.; Danilov, E. O.; Rodgers, M. A. J.; Neckers, D. C. *J. Am. Chem. Soc.* **2001**, *123*, 5136.
- (18) Hirata, Y.; Okada, T.; Mataga, N.; Nomoto, T. *J. Phys. Chem.* **1992**, *96*, 6559.
- (19) See additional discussion in the Supporting Information.
- (20) Results of TD DFT B3LYP/6-311++G(3df,2p) calculations on vertical excitation of cycloproponones **2**, **3'**, and **4** are summarized in Table S1 in Supporting Information.
- (21) Turro, N. J. *Modern Molecular Photochemistry*; University Science Books: Sausalito, CA, 1991.
- (22) The frequency of ν_{C1-C2} vibration in diphenylcycloproponone is $3.98 \times 10^{13} \text{ s}^{-1}$ according to B3LYP/6-31+G(d,p) calculations.
- (23) Serguievski, P.; Ford, W. E.; Rodgers, M. A. J. *Langmuir* **1996**, *12*, 348.
- (24) Frisch, M. J. et al. *Gaussian 98*; Gaussian, Inc., Pittsburgh, PA, 2001.
- (25) Scott, A. P.; Radom, L. *J. Phys. Chem.* **1996**, *100*, 16502.